ISSN 0016-7029, Geochemistry International, 2020, Vol. 58, No. 5, pp. 531–538. © Pleiades Publishing, Ltd., 2020.
Russian Text © The Author(s), 2020, published in Geokhimiya, 2020, Vol. 65, No. 5, pp. 464–472.

SEM Study of the Surface of Arsenopyrite and Pyrite from the Natalkinskoe Deposit, Northeastern Russia

R. G. Kravtsova[a, *], V. L. Tauson[a, **], N. A. Goryachev[a, b], A. S. Makshakov[a], K. Yu. Arsent'ev[c], and S. V. Lipko[a]

[a] *Vinogradov Institute of Geochemistry, Siberian Branch, Russian Academy of Sciences, Irkutsk, 664033 Russia*
[b] *Northeastern Complex Research Institute, Far East Branch, Russian Academy of Sciences, Magadan, 685000 Russia*
[c] *Limnological Institute, Siberian Branch, Russian Academy of Sciences, Irkutsk, 664033 Russia*
**e-mail: krg@igc.irk.ru*
***e-mail: vltauson@igc.irk.ru*

Received June 18, 2019; revised October 22, 2019; accepted October 22, 2019

Abstract—The paper presents newly acquired data on the mineral and chemical composition of the crystal surface layers of arsenopyrite and pyrite from the Natalkinskoe gold deposit, northeastern Russia. Data on arsenopyrite and pyrite grains from metasomatites and from quartz veins and veinlets were obtained using a scanning electron microscope equipped with an energy dispersive X-ray spectrometer (SEM-EDX). The surface layers of the sulfide crystals from the metasomatites contain no admixtures, except only As (up to 2.48 wt %) in the pyrite. The surface layers of arsenopyrite crystals from the vein and veinlets contains the following admixtures (wt %): Pt (up to 2.11), U (up to 2.03), Hg (up to 1.11), Au (up to 0.96), and more rarely Ru (up to 1.44), Ir (up to 0.67), Os (up to 0.64), Ag (up to 0.71), and Cu (up to 0.56). The surface layers of the pyrite crystals contain (wt %): As (up to 2.24), Pt (up to 2.88), and Cu (up to 0.69). The detected elevated concentrations of the admixtures are thought to be explained primarily by the presence of nonautonomous phases.

Keywords: arsenopyrite, pyrite, SEM-EDX, surface, microinclusions, nonautonomous phases, precious metals, Natalkinskoe gold deposit, northeastern Russia

DOI: 10.1134/S0016702920050031

INTRODUCTION

Studies of the modes in which ore elements, including precious metals, occur provide clues to understanding how ore deposits are formed and how these metals affect the quality of the ores, i.e., facilitate solving one of the principally important problems of the geochemistry of ore-forming processes. An important role is therewith played by compositional features of the surface layers of pyrite and arsenopyrite crystals, which are the dominant ore minerals at most gold deposits (Tauson et al., 2009, 2014; Tauson and Kravtsova, 2004; Kravtsova et al., 2015). The Natalkinskoe deposit is one of the largest gold deposits in Russia (Grigorov et al., 2007; Goryachev et al., 2008; and others). Along with gold, the ores of this deposit contain PGE (primarily Pt, up to a few dozen ppm, and Pd, up to a few ppm) (Voroshin et al., 1995; Goncharov et al., 2002; Plyusnina et al., 2003). However, no precious-metal minerals other than native gold and silver have ever been found at this deposit in spite of thorough targeted searches. For example, only gold microinclusions were identified on the surface of the arsenopyrite in studies with the application of the QEMSCAN (FEI Company, USA) automated analytical system (Sotskaya et al., 2012). Our earlier studies with the application of AAS (atomic absorption spectrometry), SSADSC techniques (statistical selections of analytical data on single crystals), and LA-ICP-MS (laser ablation–inductively coupled plasma–mass spectrometry) allowed us to determine that Au, Pt, and Pd occur in arsenopyrite from this deposit in two major nonmineral modes: structural and surface-related. We have proved that the high concentrations of the metals in the sulfide is explained, first of all, by the surface-related mode (Kravtsova et al., 2015). Our studies of the typomorphism (including typochemistry) of the surfaces of arsenopyrite and pyrite at the Natalkinskoe deposit were continued, and some results of these studies are presented in this publication.

MATERIALS AND METHODS

The Natalkinskoe gold deposit in the Magadan Territory, northeastern Russia, belongs to the Omchak group of placer gold deposits (Grigorov et al., 2007), is classified with the disseminated gold–sulfide type, and is thought to have been produced by a complicated

interplay of metamorphic–hydrothermal (Goncharov et al., 2002) or magmatic–hydrothermal processes with the partial remobilization of the material of the host rocks (Goryachev et al., 2008). The ores make up a structurally uniform orebody, whose inner structure is controlled by an array of long linear zones of quartz and quartz–carbonate veins and veinlets surrounded with thick aureoles of sulfidized rocks. The ores generally have a merely insignificantly varying chemical and mineralogical composition, with the only variations being those in the proportions of their components. The most widely spread sulfides at the deposit are pyrite and arsenopyrite. The ore samples from which these minerals were separated for our studies contained such non-ore minerals as carbonates, feldspars, sericite, and chlorite. In addition to pyrite and arsenopyrite (4–7%), the ores were determined to also contain galena, sphalerite, chalcopyrite, native gold, and rutile (<1%). The native gold is 750 to 900‰ fine or, more rarely, is of lower grade (electrum) and is commonly found as free large particles (0.1 to 2–3 mm) or inclusions in the gangue quartz and as aggregates with sulfides (Goncharov et al., 2002; Goryachev et al., 2008). We have studies the surfaces of twenty arsenopyrite and fourteen pyrite crystals from seven samples (8–10 kg) of the veined and string–disseminated ores with the highest gold concentrations (1.5–30.2 ppm).

It should be mentioned that the *surface* of a crystal or a crystal face is understood herein as a *layer* in which changes in the stoichiometric proportions of the mineral were detected and in which unusual *nonautonomous phases* (NPs) and products of their evolution (micrometer- and nanometer-sized inclusions) were identified (Tauson et al., 2009, 2014, 2018).

One of the methods allowing the researcher to most comprehensively study the surface of minerals is scanning electron microscopy–energy-dispersive X-ray spectrometry (SEM-EDX). The surface of arsenopyrite and pyrite crystals was studied using SEM-EDX on a FEI Company Quanta 200 scanning electron microscope equipped with an EDAX (USA) energy-dispersive X-ray spectrometer with an N-free cooling system at the Limnological Institute, Siberian Branch, Russian Academy of Sciences, analyst K.Yu. Arsent'ev. The maximum spatial resolution of the tool with a W cathode and standard detector of secondary and backscattered electrons was 3.5 nm and was 1–2 μm in analysis for chemical elements. The EDX system and the EdaxGenesis software enables not only qualitative but also quantitative analysis for a broad spectrum of elements (from Be through U) with a resolution of 127 eV and detection limits of 0.5 wt % for the elements of interest for this study. Images and analyses of the surface of the crystals were taken in high vacuum, without sputter-coating the samples, at an accelerating voltage of 30 kV. Analysis for elements was made at natural flat surface areas no smaller than 2 μm across. These surface fragments preliminarily studied under a SMM-2000 scanning electron microscope could be positioned under the electron microscope, which allowed us to select and then examine surface fragments with the minimum natural roughness, close to that of artificially polished surface (i.e., a few nanometers). Concentrations of elements were calculated using ZAF corrections. This technique involved measuring (under the same conditions) the intensity of X-ray radiation of element i of the sample J_i and a standard of known composition $J_{(i)}$, the intensity of X-ray radiation of the background was subtracted from these data, and the result was then normalized to 100%.

RESULTS AND DISCUSSION

We have studied the natural surfaces of sulfides (pyrite and arsenopyrite) of two groups (i) arsenopyrite and pyrite from the metasomatites and (ii) these minerals from the quartz veinlets and veins. For this study, we have selected euhedral pseudo-orthorhombic arsenopyrite and cubic pyrite crystals 0.5–2 mm. Our SEM-EDX data indicate that the surfaces of most of the crystals contain numerous micrometer- and submicrometer-sized inclusions of quartz, carbonate, carbonaceous matter, and more rare potassic feldspar, albite, and sericite flakes. Quartz and carbonate are quite often found as relatively large inclusions and as aggregates and thin quartz–carbonate and carbonaceous films.

On the surfaces of the minerals from the metasomatites (these minerals were classified with the first group), the dominant inclusions are non-ore minerals, first of all, quartz and carbonate grains and aggregates. Many of the films consist of quartz, quartz–carbonate, and carbonaceous matter. The films often contain micrographite. The only ore minerals are Ti oxides.

On the surface of the minerals from the ore veins and veinlets (these minerals were attributed to the second group), we identified, along with non-ore material, also ubiquitous gold, sphalerite, chalcopyrite, rutile, and more rare galena inclusions and microinclusions (Figs. 1–3). The mineral inclusions are mostly constrained within microcracks, intergranular space, and pits on the crystal faces of arsenopyrite and pyrite crystals. The mineral crystals often bear no discernible ore inclusions or microinclusions (Fig. 2). Some of the studied surfaces are variably oxidized and carbonized and show deviations in the concentration proportions of major elements from stoichiometric ones typical of these minerals (Tables 1–3). We identified gold specs of peculiar morphology (skeletal) on some faces of arsenopyrite crystals (Fig. 3). EDX analyses of the surface layer of one of such gold particles indicate that this particle is electrum (Table 1) with admixtures of U (up to 1.43), Pt (up to 0.73), and Hg (up to 0.75 wt %).

The chemical composition of the surface layers of the arsenopyrite and pyrite crystals was analyzed at preliminarily selected "clean" sites, which were prac-

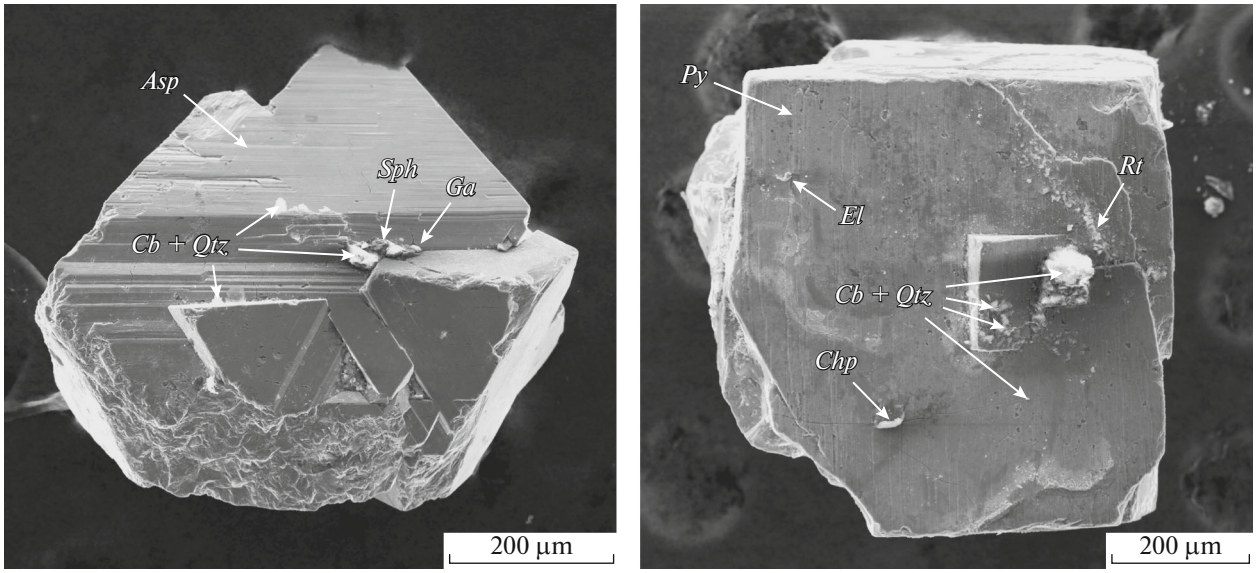

Fig. 1. Crystals of arsenopyrite (*Asp*) and pyrite (*Py*) of the second group with microinclusions of carbonate (*Cb*), quartz (*Qtz*), sphalerite (*Sph*), galena (*Ga*), electrum (*El*), chalcopyrite (*Chp*), and rutile (*Rt*) from the ore-bearing veinlets and veins. Here and below, the micrographs are secondary-electron images.

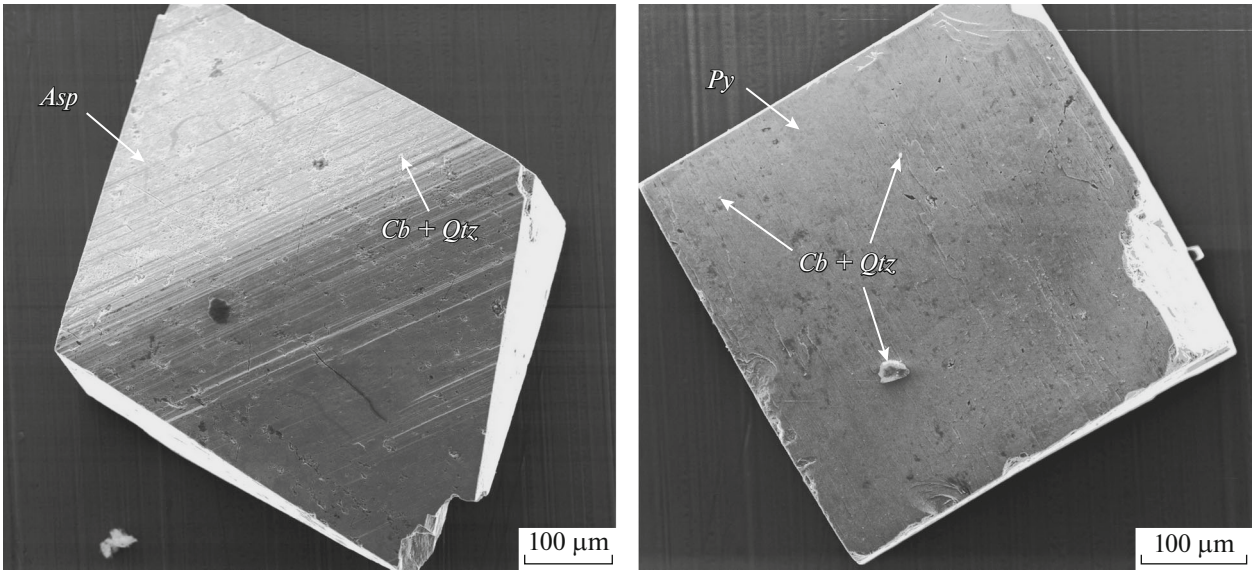

Fig. 2. Crystals of arsenopyrite (*Asp*) and pyrite (*Py*) of the second group with microinclusions of carbonate (*Cb*) and quartz (*Qtz*) from ore-bearing veinlets and veins.

tically absolutely devoid of discernible inclusions and significant defects (Fig. 4). These sites were 10 × 10, 20 × 20, and 30 × 30 μm. In order to rule out the effect of admixtures captured by the growing faces of different type of the crystals, scanning was carried out on striated faces of prism {141} for arsenopyrite and cube {100} for pyrite. The composition of the surface layer at these is reported in Tables 2 and 3.

The surface layer of the group-I arsenopyrite contained no identifiable ore elements in concentration higher than 0.5 wt %, and the pyrite of this group always contains only an admixture of As (up to 2.48 wt %). The surface layers of the group-II arsenopyrite and pyrite shows certain clearly seen distinguishing features (typomorphism of the surface). For example, the surface layer at sites of "clean" surface (i.e., without dis-

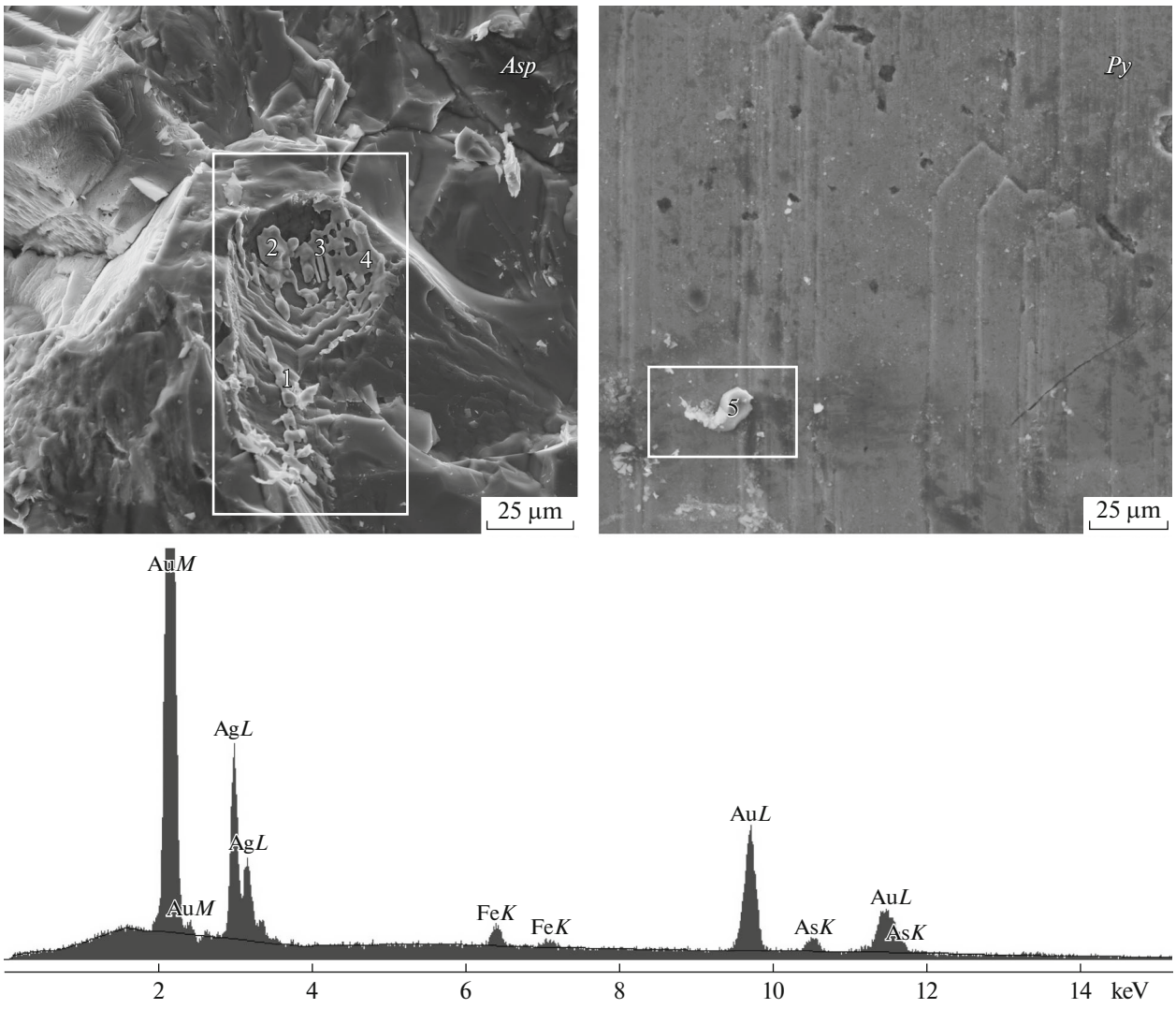

Fig. 3. Fragments of the surface of arsenopyrite (*Asp*) and pyrite (*Py*) crystals of the second group from ore-bearing veinlets and veins. The rectangular contour in the left-hand image outlines an aggregate of gold (electrum), quartz, and carbonate. The right-hand image is an enlarged fragment is the pyrite crystal shown in Fig. 1 with an electrum inclusion. 1–5 are analytical spots (see Table 1). The X-ray energy-dispersive spectra are presented below (spot 5).

cernible inclusions of ore minerals) of the arsenopyrite of this group contains admixtures (wt %) of Pt (up to 2.11), U (up to 2.03), Hg (up to 1.11), Au (up to 0.96), and more rare Ru (1.44), Ir (up to 0.67), and Os (up to 0.64), and occasionally also Ag (up to 0.71) and Cu (up to 0.56) (Table 2). The surface layer of pyrite of this group contains (wt %) As (up to 2.24), Pt (up to 2.88), and Cu (up to 0.69) (Table 3).

Analysis of data on the admixtures puts forth the problem of their nature and a possible explanation of relatively little varying Al concentration on the surface of the pyrite (and to a lesser degree, also the arsenopyrite). A possible reason for this is that the surface layer contains submicrometer-sized nonautonomous phases containing Al and other incompatible elements. Experimental data (Tauson et al., 2017) suggest that Al and Fe^{3+} may occur in a sulfoxide form (sulfate, thiosulfate) in the NP. At the same time, our earlier XPS and AES data indicate that the surface of pyrite is partly covered by submicrometer-sized (~0.5 μm) films containing lithophile elements: Al, Si, and K (Tauson and Kravtsova, 2004). However, Al does not clearly correlate with Si and K in our situation within the stoichiometric proportions of their probable common phases (sericite, adularia, etc.), and this issue requires further XPS and AES studies to distinguish between Al in an individual oxide phase and in an sulfoxide NP (Tauson et al., 2017).

The idea that arsenopyrite and pyrite can concentrated PGE at the Natalkinskoe deposit was suggested in (Plyusnina et al., 2003), who continued the studies (Voroshin et al., 1995). It was later found out that,

Table 1. Chemical composition (wt %) of the surface layer of a skeleton electrum inclusion (spots 1–4) on the surface of an arsenopyrite crystal and an electrum grain (spot 5) on the surface of As-bearing pyrite, Natalkinskoe deposit

n	Au	Ag	C	O	Fe	As	Hg	Pt	Os	Ir	Rh	U
1	**48.65**	**33.42**	6.23	2.60	3.30	4.00	0.66	0.62	*0.33*	*0.33*	*0.16*	0
2	**48.92**	**32.67**	7.83	2.64	2.92	4.07	0	0	0	0	*0.11*	0.84
3	**46.97**	**33.91**	7.53	2.58	2.97	4.09	*0.31*	*0.42*	0	0	*0.10*	1.12
4	**49.21**	**33.41**	5.65	2.65	0.80	4.77	0.75	0.73	*0.30*	*0.30*	0	1.43
5	**58.61**	**36.35**	0	0	1.27	3.77	0	0	0	0	0	0

n is the analytical spots. Here and in Tables 2 and 3 below, the totals are normalized to 100%, the concentrations of the dominant elements are printed in bold, concentrations below the EDX detection limits (<0.5 wt %) are printed in italics, zero means not detected. Analytical lines: AuL_α, AgL_α, CK_α, OK_α, FeK_α, AsK_α, HgL_α, PtL_α, OsL_α, IrL_α, RhL_α, and UL_α. The high Fe and As concentrations are most likely explained by the effects of the matrix (arsenopyrite or pyrite for spot *5*).

Table 2. Chemical composition (wt %) of the surface layers of the arsenopyrite and pyrite crystals with micrometer-sized inclusions of non-ore minerals on the surface (*1–5*). Natalkinskoe deposit

N	*n*	Fe	As	S	C	O	Al	Si	K	Na	Hg	Au	Ag	Cu	Ti	Pt	Os	Ir	Ru	U
Arsenopyrite, group I																				
1	1	**29.35**	**34.68**	**23.17**	1.62	7.85	1.31	*0.48*	0.75	0.57	0	0	0	0	*0.22*	0	0	0	0	0
	2	**28.96**	**33.69**	**22.07**	5.29	5.83	3.02	0.66	0	*0.48*	0	0	0	0	0	0	0	0	0	0
2	1	**29.84**	**34.13**	**24.76**	2.73	2.48	5.01	*0.26*	*0.07*	0.66	0	0	0	0	*0.06*	0	0	0	0	0
	2	**28.24**	**32.34**	**22.81**	4.71	5.19	4.97	0.91	*0.16*	0.60	0	0	0	0	*0.07*	0	0	0	0	0
3	1	**32.95**	**35.70**	**20.20**	3.55	4.86	1.74	*0.39*	*0.13*	*0.39*	0	0	0	0	*0.09*	0	0	0	0	0
	2	**33.98**	**38.65**	**21.30**	1.90	1.43	1.88	*0.28*	*0.10*	*0.43*	0	0	0	0	*0.05*	0	0	0	0	0
4	1	**31.56**	**40.95**	**16.23**	4.54	4.46	1.22	*0.32*	0	0	0	0	*0.25*	*0.30*	*0.17*	0	0	0	0	0
	2	**31.66**	**41.52**	**17.11**	2.09	5.04	1.89	*0.23*	0	0	0	0	0	*0.30*	*0.16*	0	0	0	0	0
5	1	**25.86**	**28.71**	**23.27**	5.61	4.55	10.22	0.64	*0.17*	0.54	0	0	0	*0.32*	*0.11*	0	0	0	0	0
	2	**21.29**	**21.68**	**17.33**	6.52	17.85	8.31	5.48	0.75	0.57	0	0	0	0	*0.22*	0	0	0	0	0
Arsenopyrite, group II																				
6	1	**31.59**	**35.96**	**23.39**	2.82	2.04	1.22	*0.16*	0	0	0.65	0.67	*0.23*	0	0	*0.47*	0	0	0	0.80
	2	**32.46**	**35.65**	**20.18**	3.39	2.49	1.27	*0.21*	0	0	1.08	0.86	*0.31*	0	0	0.61	0	0	0	1.49
	3	**31.89**	**36.76**	**20.76**	3.67	1.52	0.60	*0.15*	0	0	1.05	0.94	*0.28*	0	0	0.78	0	0	0	1.60
7	1	**29.99**	**36.32**	**20.43**	4.31	2.44	1.17	*0.11*	0	0	1.11	0.93	*0.11*	0	0	1.05	0	0	0	2.03
	2	**28.86**	**39.01**	**20.63**	4.55	2.52	0.54	*0.18*	0	0	0.86	0.78	*0.24*	0	0	*0.44*	0	0	0	1.39
8	1	**32.64**	**41.75**	**16.13**	3.94	1.51	0	0	0	0	0.95	0.67	0	0	0	0.54	0.57	*0.44*	0	0.86
	2	**32.13**	**43.39**	**14.20**	2.33	1.39	0	0	0	0	0.87	0.96	*0.21*	0	0	0.95	0.64	0.67	0.97	1.29
	3	**32.34**	**43.08**	**15.43**	1.08	1.01	0	0	0	0	0.91	0.94	0.71	0	0	0.92	0.67	0.69	1.02	1.20
9	1	**34.02**	**40.16**	**15.11**	4.59	2.70	0	0	0	0	*0.49*	*0.26*	0	0	0	*0.37*	*0.14*	*0.29*	1.44	*0.43*
	2	**34.69**	**41.47**	**13.75**	4.75	1.75	0	0	0	0	*0.48*	*0.46*	0	0	0	*0.36*	*0.21*	*0.24*	1.24	0.60
10	1	**30.79**	**41.18**	**17.08**	3.95	3.22	1.02	*0.09*	0	0	0	0	0	0.56	0	2.11	0	0	0	0
	2	**31.91**	**41.72**	**19.02**	1.90	2.11	1.38	*0.08*	0	0	0	0	*0.12*	0.52	*0.14*	1.10	0	0	0	0

No Pd, Rh, F, Cl, Pb, Zn, Mo, W, Bi, and REE were detected. Here and in Table 3, *N* is the sequential number of the crystal, and *n* is the sequential number of the analytical site. Analytical lines: FeK_α, AsK_α, SK_α, CK_α, OK_α, AlK_α, SiK_α, KK_α, NaK_α, HgL_α, AuL_α, AgL_α, CuK_α, TiK_α, PtL_α, OsL_α, IrL_α, RuL_α, and UL_α.

along with Au, elevated Pt and Pd concentrations occur at the Natalkinskoe deposit in arsenopyrite. According to electrothermal atomic absorption spectrometric data (*Determining Au, Pt, Pd...,* 2005), Pt concentration in monomineralic fractions of this sulfide vary from 23.0 to 62.4 ppm, and the Pd concentrations are 2.3–9.5 ppm (Kravtsova et al., 2015). Our studies of the arsenopyrite with the application of this technique allowed us to detect, along with Pt and Pd, also Ru and Rh. Our newly obtained data on the arse-

Table 3. Chemical composition (wt %) of the surface layers of the pyrite crystals with micrometer-sized inclusions of non-ore minerals on the surface. Natalkinskoe deposit

N	*n*	Fe	S	C	O	Al	Si	Ca	Na	K	As	Cu	Ti	Pt
Pyrite, group I														
1	1	**41.94**	**43.67**	6.37	4.38	1.09	0.81	*0.15*	0	*0.09*	1.43	0	*0.07*	0
	2	**39.52**	**46.54**	4.24	6.38	0.92	*0.39*	*0.15*	0	*0.13*	1.62	0	*0.11*	0
2	1	**45.40**	**40.04**	3.88	4.94	2.47	*0.33*	*0.14*	*0.18*	*0.13*	2.32	0	*0.17*	0
	2	**42.42**	**33.20**	4.51	11.72	3.88	1.09	*0.32*	*0.08*	*0.19*	2.48	0	*0.11*	0
	3	**42.91**	**39.40**	4.40	7.17	2.18	0.81	*0.28*	*0.15*	*0.27*	2.13	0	*0.30*	0
3	1	**38.54**	**51.21**	2.49	4.60	0.86	*0.17*	*0.27*	*0.19*	*0.26*	1.17	0	*0.24*	0
	2	**38.46**	**50.50**	3.31	3.98	0.82	*0.31*	*0.36*	0	*0.37*	1.55	0	*0.34*	0
4	1	**38.81**	**45.78**	5.56	7.07	1.05	*0.41*	*0.11*	0	*0.10*	0.98	0	*0.13*	0
	2	**38.70**	**45.78**	6.64	6.37	1.23	*0.33*	*0.04*	0	*0.05*	0.81	0	*0.05*	0
5	1	**37.96**	**46.14**	7.64	5.31	0.91	*0.40*	*0.09*	0	*0.10*	1.22	0	*0.23*	0
	2	**39.57**	**50.04**	3.42	4.22	0.81	*0.20*	*0.09*	0	*0.11*	1.39	0	*0.15*	0
	3	**34.13**	**42.09**	7.99	11.44	1.37	1.29	*0.09*	*0.08*	*0.20*	1.26	0	*0.06*	0
Pyrite, group II														
6	1	**38.48**	**43.12**	5.26	7.74	1.21	*0.23*	0	0	0	1.35	0.69	*0.25*	1.67
	2	**36.89**	**39.22**	7.02	10.74	1.29	*0.36*	0	0	0	1.17	0.66	*0.36*	2.29
	3	**40.96**	**47.87**	2.90	2.62	1.40	*0.18*	0	0	0	1.71	0.51	*0.21*	1.64
7	1	**39.82**	**44.13**	5.03	6.78	1.13	*0.20*	0	0	0	1.03	0	*0.16*	1.72
	2	**35.87**	**42.70**	5.59	10.21	0.78	1.10	0	0	0	1.05	0.58	*0.16*	1.96
	3	**38.80**	**46.97**	3.30	6.15	0.93	0.88	0	0	0	1.11	*0.31*	*0.12*	1.43
8	1	**37.02**	**38.32**	4.32	13.21	0.93	0.72	*0.20*	*0.26*	0	1.76	0.54	0	2.72
	2	**39.48**	**48.38**	2.28	3.04	0.85	*0.08*	*0.05*	*0.20*	0	2.24	0.52	0	2.88
9	1	**37.35**	**37.48**	3.10	16.39	1.33	1.02	0	0	0	1.14	*0.38*	*0.12*	1.69
	2	**40.55**	**46.49**	3.56	5.64	1.38	*0.13*	0	*0.17*	0	1.38	*0.16*	0	0.54
10	1	**41.69**	**47.16**	2.55	3.34	0.94	*0.12*	0	0	0	2.00	*0.27*	0	1.93
	2	**40.70**	**47.51**	3.00	4.05	0.85	*0.16*	0	0	0	2.02	*0.25*	0	1.46

No Au, Ag, Hg, Pd, Os, Ir, Ru, Rh, U, F, Cl, Pb, Zn, Mo, W, Bi, and REE were detected. Analytical lines: FeK_α, SK_α, CK_α, OK_α, AlK_α, SiK_α, CaK_α, NaK_α, KK_α, AsK_α, CuK_α, TiK_α, and PtL_α.

nopyrite monomineralic separates indicate that the mineral contains up to 119.9 ppm Pt and 9.5 ppm Pd, whereas the pyrite contains up to 25.3 ppm Pt and up to 5.8 ppm Pd. The highest Ru and Rh concentrations were found in the arsenopyrite: 66.8 and 21.4 ppm, respectively, whereas the pyrite contains 52.5 and 15.2 ppm, respectively. The recently acquired data are in good agreement with our earlier results (Kravtsova et al., 2015) and do not contradict data of other researchers on Pt concentrations up to tens of ppm and Pd concentrations up to a few ppm in the ores (Goncharov et al., 2000, 2002; Plyusnina et al., 2003). Interesting data on PGE concentrations close to our values for sulfide monomineralic fractions were published in (Mitkin et al., 2000). The following PGE concentrations (ppm) were determined in the Au-bearing (up to 1476 ppm Au) gravity concentrates of the sulfides: Pt (up to 92.80), Pd (up to 2.97), Ru (up to 0.29), Rh (up to 0.95), and Ir (up to 0.30).

These are fairly high concentrations of the precious metals, which have not been determined by EMP analysis in "normal" pyrite and arsenopyrite samples (Goncharov et al., 2002) and seem to be explained by the occurrence of NPs responsible for concentrating Au at the surface of pyrite at deposits of various types (Tauson and Kravtsova, 2004; Tauson et al., 2009, 2014). The presence of such phases was proved for arsenopyrite at the Natalkinskoe deposit (Kravtsova et al., 2015). This is consistent with information that the highest PGE concentrations at the Natalkinskoe deposit occur in quartz–sulfide ores (Gonsharov et al., 1995; Voroshin et al., 1995). It is thought that the same uptake mechanism of admixture elements operates for both arsenopyrite and pyrite and is driven by an active role of crystal surfaces and surface defects and by unusual phases: nonautonomous phases and their evolution products (micro- and nanometer-sized inclusions) (Tauson et al., 2018).

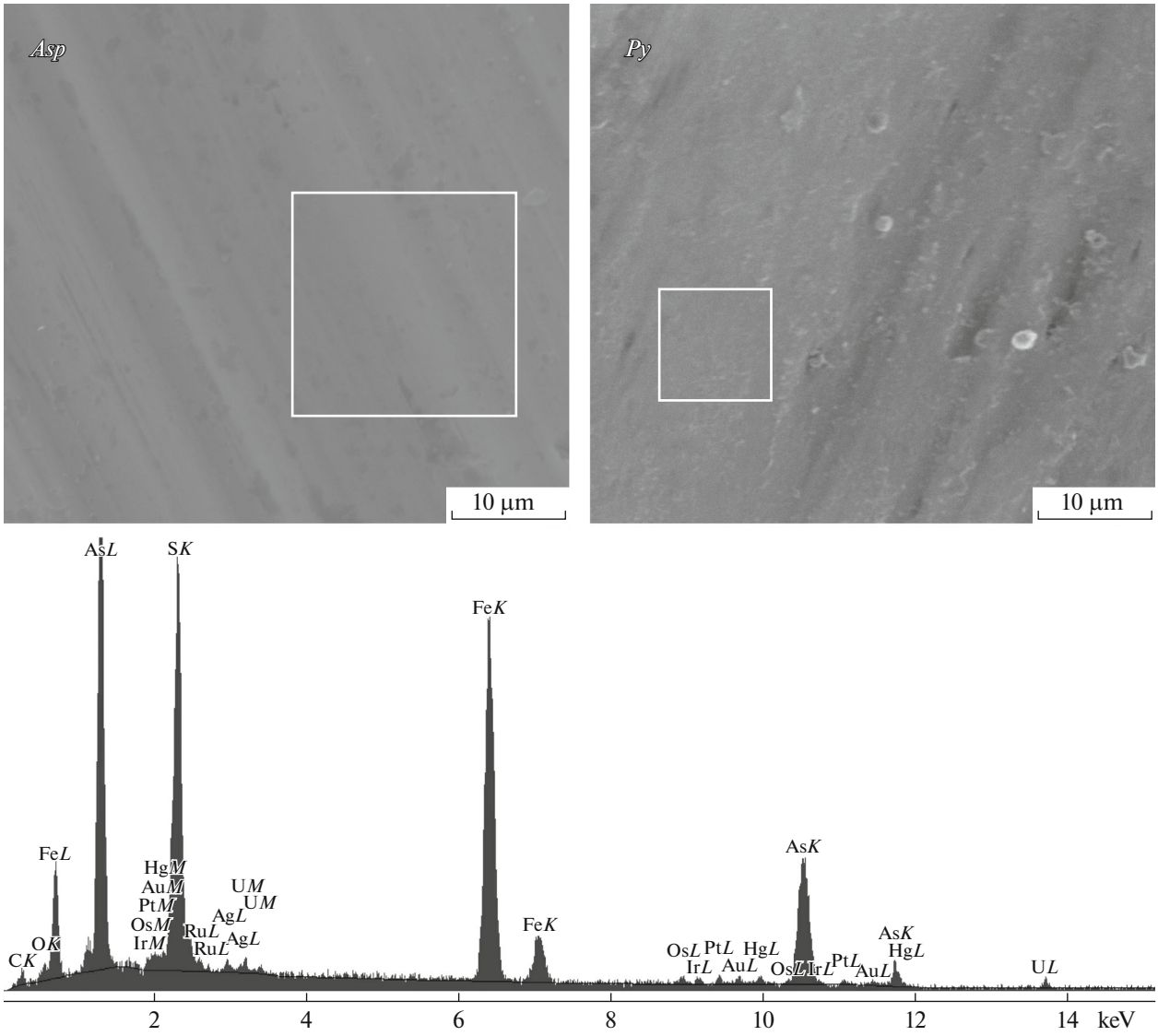

Fig. 4. Enlarged surface fragments of crystals of arsenopyrite (*Asp*) and pyrite (*Py*) of the second group (from ore-bearing veinlets and veins) with "clean" sites at which the measurements were made (see Table 2, N *8*, n *3* and Table 3, N *6,* n *2*). The X-ray energy-dispersive spectra of the arsenopyrite are presented below (see Table 2, N *8*, n *3*).

CONCLUSIONS

SEM-EDX data on arsenopyrite and pyrite crystals from the Natalkinskoe gold deposit show that the composition of the natural surface layers of these minerals is different for sulfides from the metasomatites and those from the quartz veins and veinlets. The surface layers of arsenopyrite and pyrite crystals from the metasomatites only very rarely bears inclusions of ore minerals, and inclusions in these layers are mostly Ti oxides. No admixtures of ore elements have been detected. Pyrite from the metasomatites is noted for always containing As (up to 2.48 wt %). The surface of arsenopyrite and pyrite crystals from the veins and veinlets contains small and fine inclusions of gold, sphalerite, chalcopyrite, and galena. The surface layer of the arsenopyrite crystals contains admixtures (in wt %) of Pt (up to 2.11), U (up to 2.03), Hg (up to 1.11), Au (up to 0.96), Ru (1.44), Ir (up to 0.67), Os (up to 0.64), and more rare Ag (up to 0.71), and Cu (up to 0.56), whereas the surface layer of the pyrite contains As (up to 2.24), Pt (up to 2.88), and Cu (up to 0.69).

The same mechanism of precious-metal accumulation (in the form of admixtures) seems to operate for both arsenopyrite and pyrite from the ore-bearing veins and veinlets. This mechanism is related to an active role of the surfaces of the crystals. The reasons for enrichment of the elements in the surface layers are the growth specifics of the crystals by means of NP and the dualism in the distribution coefficients of the elements in the mineral–hydrothermal solution system: these coefficients are as much as one order of

magnitude higher for the NPs than for the rest of the crystal volume. This is consistent with experimental data on the modes in which Pt is accommodated in pyrite crystals growing in hydrothermal environments. When a crystal grows, NPs aggregate into submicrometer- and micrometer-sized crystals that inherit an unusual admixture-composition from the NPs and bear elevated concentrations of precious metals and other admixtures (Tauson et al., 2018). The role of the surface layer, which is modified into NPs of complicated composition, seems to explain the anomalous PGE concentrations found in the ores of the Natalkinskoe deposit.

ACKNOWLEDGMENTS

This study was carried out using equipment of the Collective-Use Center for Isotope–Geochemical Studies at the Vinogradov Institute of Geochemistry, Siberian Branch, Russian Academy of Sciences, and the Collective-Use Center for Ultramicroanalysis at the Limnological Institute, Siberian Branch, Russian Academy of Sciences.

FUNDING

This study was carried out under government-financed program IX.125.3.4 (0350-2019-0003) and was supported by the Russian Foundation for Basic Research, project nos. 17-05-00095, 18-05-00077, and by project 0350-2018-0001, MP SB RAS.

REFERENCES

Determination of Gold, Platinum, Palladium, Rhodium, Iridium, Ruthenium in Rocks Using Atomic Absorption with Electrothermal Atomization after Preconcentration. Method NSAM no. 430-X (VIMS, Moscow, 2005) [in Russian].

V. I. Goncharov, S. V. Voroshin, and V. A. Sidorov, "Platinum potential of gold deposits in black shales of Northeast Russia: problems and prospects," *Platinum of Russia, Problems of Development of PGM Mineral-Raw Base. Proceedings of 3rd Session of Research-Methodical Council in the Program "Platinum of Russia,"* (Geoinformmark, Moscow, 1995), Vol. 2, book 2, pp. 156–161.

V. I. Goncharov, V. A. Sidorov, and V. A. Pristavko, "PGM potential of the Natalka deposit: summary of studies," Kolyma, No. 2, 49–53 (2000).

V. I. Goncharov, S. V. Voroshin, and V. A. Sidorov, *Natalka Gold Deposit* (SVKNII DVO RAN, Magadan, 2002) [in Russian].

N. A. Goryachev, O. V. Vikent'eva, N. S. Bortnikov, V. Yu. Prokof'ev, V. A. Alpatov, and V. V. Golub, "The world-class Natalka Gold Deposit, Northeast Russia: REE patterns, fluid inclusions, stable oxygen isotopes, and formation conditions of ore," Geol. Ore Deposits **50** (5), 362–390 (2008).

S. A. Grigorov, V. D. Vorozhbenko, P. I. Kushnarev, V. Yu. Makarevich, V. N. Tokarev, V. I. Chichev, N. P. Yagubov, and B. K. Mikhailov, "Natalka gold deposit: structure and main prospecting indicators," Otechestvennaya Geol., No. 3, 43–50 (2007).

R. G. Kravtsova, V. L. Tauson, and E. M. Nikitenko, "Modes of Au, Pt, and Pd Occurrence in arsenopyrite from the Natalkinskoe deposit, NE Russia," Geochem. Int. **53** (11), 964–972 (2015).

V. N. Mitkin, A. A. Galizky, and T. M. Korda, "Some observations on the determination of gold and the platinum-group elements in black shales," Geostand. Newslet. **24** (2), 227–240 (2000).

L. P. Plyusnina, A. I. Khanchuk, V. I. Goncharov, V. A. Sidorov, N. A. Goryachev, T. V. Kuz'mina, and G. G. Likhoidov, "Gold, platinum, and palladium in ores of the Natalka Deposit, Upper Kolyma region," Dokl. Earth Sci. **391A** (6), 836–840 (2003).

O. Sotskaya, N. Goryachev, E. Goryacheva, and E. Nikitenko, "Micromineralogy of "Black Shale" Disseminated-Sulphide Gold Ore Deposits of the Ayan-Yuryakh Anticlinorium (North-East of Russia)," Int. J. Earth Sci. Eng., No. 2, 744–753 (2012).

V. L. Tauson and R. G. Kravtsova, "Chemical typomorphism of mineral surfaces: surface composition specifics (by the example of gold-bearing pyrite from epithermal deposit)," Russ. Geol. Geophys. **45** (2), 204–208 (2004).

V. L. Tauson, R. G. Kravtsova, V. I. Grebenshchikova, E. E. Lustenberg, and S. V. Lipko, "Surface typochemistry of hydrothermal pyrite: electron spectroscopic and scanning probe microscopic data. II. Natural pyrite," Geochem. Int. **47** (3), 231–243 (2009).

V. L. Tauson, R. G. Kravtsova, N. V. Smagunov, A. M. Spiridonov, V. I. Grebenshchikova, and A. E. Budyak, "Structurally and superficially bound gold in pyrite from deposits of different genetic types," Russ. Geol. Geophys. **55** (2), 273–289 (2014).

V. L. Tauson, S. V. Lipko, K. Y. Arsent'ev, Y. L. Mikhlin, D. N. Babkin, N. V. Smagunov, T. M. Pastushkova, I. Y. Voronova, and O. Y. Belozerova, "Dualistic distribution coefficients of trace elements in the system mineral-hydrothermal solution. IV. Platinum and silver in pyrite," Geochem. Int. **55**(9), 753–774 (2017).

V. L. Tauson, S. V. Lipko, N. V. Smagunov, and R. G. Kravtsova, "Trace element partitioning dualism under mineral–fluid interaction: origin and geochemical significance," Minerals **8** (7), 282 (2018).

V. L. Tauson, S. V. Lipko, N. V. Smagunov, R. G. Kravtsova, and K. Yu. Arsent'ev, "Distribution and segregation of trace elements during the growth of ore mineral crystals in hydrothermal systems: geochemical and mineralogical implications," Russ. Geol. Geophys. **59** (12), 1718–1732 (2018).

S. V. Voroshin, V. A. Sidorov, and E. E. Tyukova, "PGE geology, geochemistry, and prospects of the Natalka gold deposit, Northeast Russia," *Platinum of Russia, Problems of Development of PGM Mineral-Raw Base. Proceedings of 3rd Session of Research-Methodical Council in the Program "Platinum of Russia,"* (Geoinformmark, Moscow, 1995), Vol. 2, book 2, pp. 161–176 [in Russian].

Translated by E. Kurdyukov